

Epitaxial Growth in Polymers (A survey of polymer crystallization by X-ray diffraction . chapter 8)

メタデータ	言語: en 出版者: SKP 公開日: 2008-01-31 キーワード (Ja): キーワード (En): 作成者: Asano, Tsutomu, Mina, Md. Forhad メールアドレス: 所属:
URL	http://hdl.handle.net/10297/555

Chapter 8. Epitaxial Growth in Polymers

8.1 Introduction

Epitaxial crystallization has its origin in particular interactions between interfaces of different polymers. In other words, during epitaxial growth a surface of one polymer will affect to the adjacent surface of another polymer with spatial relations. When the base-polymer is highly oriented, the epitaxial polymer reveals a unique orientation. Heteroepitaxy is a well-known phenomenon of surface-induced polymer crystallization between different polymers [1-8]. Homoepitaxy (self-epitaxy) is the crystallization between the same polymer. The α -phase polypropylene (α -PP) has a cross-hatched texture [9]. In the oriented α -PP, perpendicular crystal is formed by the self-epitaxy [5] (See also Chapter 5, pp67).

As an example of the epitaxial crystallization, we refer to a blend of polyoctenamer (TOR) and α -PP [10,11]. A TEM micrograph of TOR epitaxy on the highly oriented α -PP is illustrated in Figure 8.1(a). A cross-hatched surface of TOR lamellae are inclined with the direction of PP molecules i.e. with the direction of the arrow. A schematic model of a layer structure is shown in Fig.8.1(b). As a base texture, the oriented α -PP has a stacked lamellar arrangement with an alternating sequence of crystalline region and amorphous parts. (In the very thin PP film, the above self-epitaxy is not observed.) The TOR lamellae, which look like thin fibrils in Fig.8.1a, are inclined (average 40°) from the PP molecular direction. As a result of the epitaxial crystallization, fracture stress of the blend film is increased. The morphology of PP can be reinforced by stiff TOR lamellae that can bridge the amorphous PP layers [11].

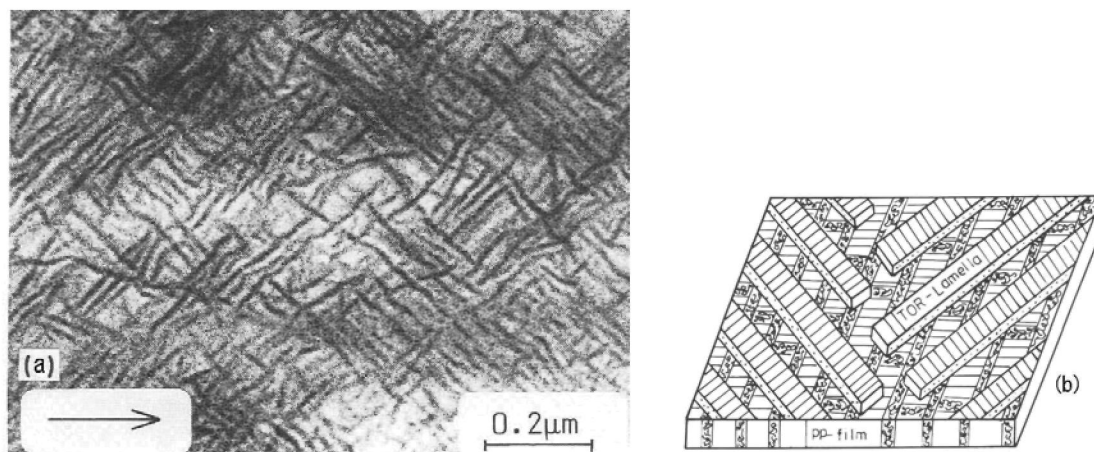


Fig. 8.1 (a) TEM micrograph of PP/TOR blends (The arrow indicates the molecular direction of PP). (b) A schematic sketch of a layer structure after the epitaxial crystallization.[11]

Much attention is paid for the blend of polypropylene and polyethylene (PP/PE) film. On the fitting surface, zigzag chains of PE with two-fold symmetry and the helical PP molecules are epitaxially crystallized, in which the zigzag chains are inclined $\pm 50^\circ$ to the PP

chain direction. This kind of orientational relationship was explained in terms of the parallel alignment of the zigzag chains along methyl group rows in the (010) lattice plane of α -PP with a 0.5 nm intermolecular chain distance for chain-row matching shown in Fig.8.2. The effect of the matching is widely observed in the several pairs including PP/TOR [3-11].

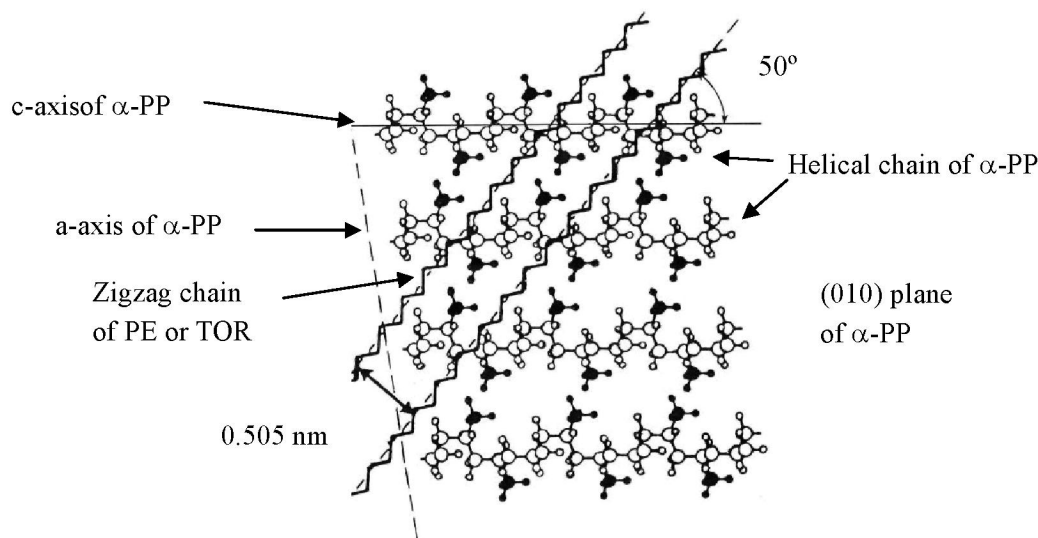


Fig. 8.2 Schematic illustration of epitaxial contact between PP and PE (or TOR)
The black parts on α -PP indicate the protruding CH_3 groups.

Most epitaxial phenomena were observed by TEM or electron diffraction using monolayer systems [3-8]. The ordinal film used in TEM is in the order of 0.1 μm . The contact plane with PP and PE was single, and the resultant crystal was laterally developed along the interfacial surface. In order to examine the bulk effect, multilayered PP/PE films were examined by X-ray diffraction. It is possible to analyze crystallization along the thickness (perpendicular to the contact plane). The *in situ* process was also observed during the epitaxial development [12].

8.2 Preparation and characterization of epitaxial samples

Uniaxially oriented thin films of HDPE (High density polyethylene) and α -PP were prepared by the following method [13]: A small amount of a 0.5 wt%-solution of the polymer (HDPE or PP) in xylene was poured and uniformly spread on a preheated glass plate, where the solvent was allowed to evaporate. After evaporating the solvent, the remaining polymer film was picked up by a motor driven cylinder with a drawing speed of 20 cm/s. The highly oriented PP or HDPE film, about 30 ~ 50 nm thick, were stacked alternately for about 5000 layers and subjected to a pressure of 5 Pa at 120 $^{\circ}\text{C}$ (below the melting temperatures of PP and HDPE), improving the contact of the films. The resulting specimen, with thickness 0.2 to 0.25 mm, was used for the X-ray measurements.

Structural measurements were performed by WAXS and SAXS using an imaging plate (IP). In order to discuss a specific orientation of the crystallized textures, WAXS and SAXS patterns were detected in three directions. We define here Cartesian coordinates (Fig. 8.3), where x-axis is perpendicular to the film surface, y-axis is perpendicular to the draw direction, and z-axis is parallel to the draw direction. Considering the beam directions, the X-ray

patterns are named as follows:

1. “Through” pattern: the incident X-ray parallel to the x-axis.
2. “Edge” pattern: the incident X-ray parallel to the y-axis.
3. “End” pattern: the incident X-ray parallel to the z-axis.

In order to perform partial heating in the isothermal condition, we tried to heat samples using a DSC. To avoid shrinkage during the heating, the original sample was wound on a thin aluminum plate (3.5 mm × 3.5 mm) made of the cover plate of the DSC pan. The sample was heated at 1 °C/min without shrinkage up to the annealing temperature 140 °C (lower than the melting temperature of iPP, and higher than that of HDPE) and was maintained for 20 min. Then, the sample was cooled in the DSC by 2.5 °C/min to a setting temperature (for example, 80 °C: lower than the crystallizing temperature of PE). Most of the X-ray measurements were performed at room temperature.

Moreover, the *in situ* WAXS and SAXS measurements were performed using synchrotron radiation. For preventing shrinkage during heating, the oriented sample was sandwiched between two metal plates, which have a hole for passing the X-ray beam.

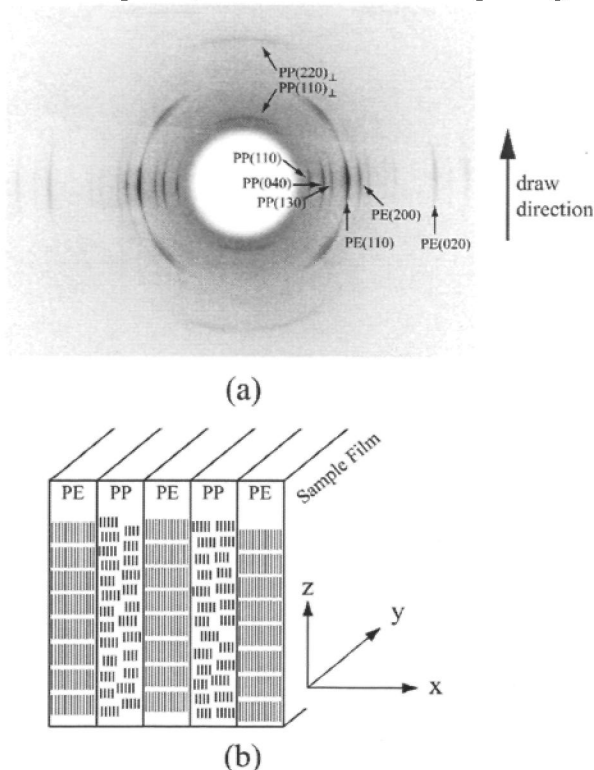


Fig. 8.3 (a) WAXS pattern and (b) molecular and lamellar orientation of PP/HDPE film before heating.[12]

8.3 X-ray diffraction studies

8.3.1 Structure of the oriented PP/HDPE film

WAXS and SAXS measurements of the original sample before heating were carried out at room temperature. In Fig.8.3(a), $hk0$ reflections of both PP and PE are aligned on the equator, indicating that c -axes are oriented along the draw direction. From these results, a schematic picture of the original sample is illustrated in Fig. 8.3(b).

In Fig.8.3(a), the PP (110) and (220) reflections appear near the meridian. These

reflections indicate the existence of the a^* -orientation of α -phase PP crystal due to the self-epitaxy [5, 9], considered to be a secondary crystallization of PP onto the c -axis oriented α -PP. As a result of the a^* -orientation, the c -axis becomes perpendicular to the draw-direction. From these results, we consider both epitaxial growths of PE onto the c -axis and a^* -axis oriented α -PP.

The SAXS pattern of the original sample indicates that the lamellar normals of PP and PE are parallel to the z -axis. The thickness of the PE lamellae is detected as 27 nm, while PP shows a dispersed lamellar structure (average 16 nm) thinner than PE.

8.3.2 *In situ* SAXS and WAXS measurements

All patterns in this measurement were “through” pattern, because the incident X-ray beam was perpendicular to the sample film. The film was heated to 150 °C without shrinkage. After holding this temperature for 10 min, the X-ray WAXS and SAXS patterns were simultaneously measured for 5 min (Figs.8.4 (a) and (d)). Then, the samples were cooled by 2 °C/min to 80 °C. Simultaneous measurements were performed on the cooling process from 121 to 111 °C, and from 90 to 80 °C.

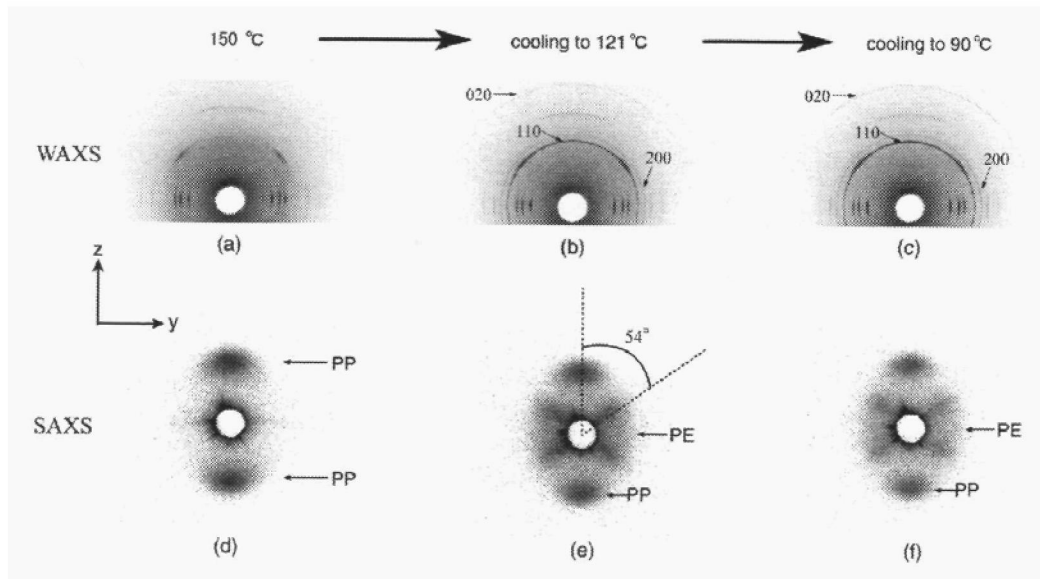


Fig. 8.4 Through patterns by *in situ* measurements of WAXS at (a) 150 °C and (b), (c) during cooling; SAXS at (d) 150 °C and (e), (f) during cooling.[12]

Fig.8.4(a) and (d) correspond to the WAXS and SAXS reflections from the oriented α -phase without any PE reflections. By heating to 150 °C, the PP lamellae are grown to 21 nm [Fig.8.4(d)]. Reflections from the PE crystal appear during cooling from 121 to 111 °C. The SAXS pattern indicates that PE lamellae are developed at an angle of 54° from the z -axis [Figs.8.4(e) and (f)]. In Figs.8.4(b) and (c), the WAXS PE reflections (110, 200 and 020) are spread on broad arcs. As the PE reflections appear in Figs.8.4(c) and maintain in Fig.8.4(d), crystallization of PE mainly develops during the cooling process to 111 °C.

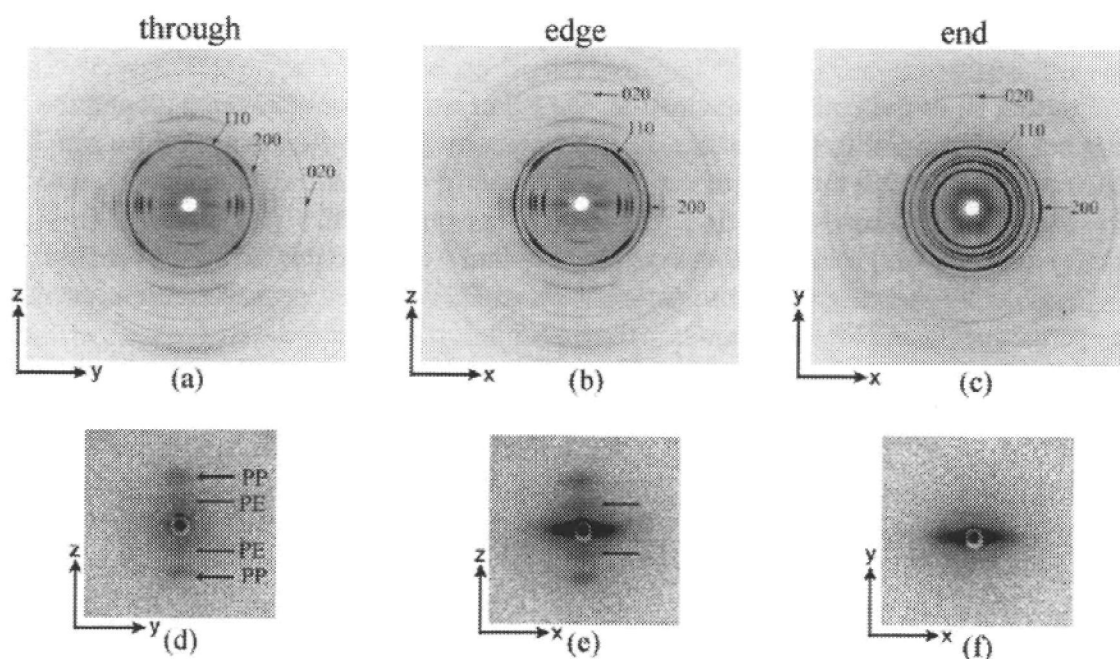


Fig. 8.5 WAXS (a, b and c) and SAXS (d, e and f) patterns by three different incident directions. The sample was annealed at 140 °C in the DSC, and then cooled to room temperature by 2.5 °C/min.[12]

8.3.3 Three dimensional analysis

For precise analysis of the PP/HDPE sample, it is necessary to execute three-dimensional observations. The original sample was heated without shrinkage to 140 °C (above the melting temperature of HDPE) in DSC. Then it was cooled to room temperature for WAXS and SAXS measurements.

The results are shown in Fig. 8.5. In the WAXS “through” pattern [Fig.8.5(a)], PE 110, 200, and 020 reflections spread on arcs showing random orientation in the through direction. PE 020 is located on the meridian in Fig.8.5(b). The “end” pattern in Fig.8.5(c) has oriented 110, 200, and 020 reflections.

Summarizing these results, the a -axis of PE is oriented parallel to the x -axis, and the b -axis is distributed along the yz -plane. On the SAXS “edge” and “end” patterns, a strong streak appears along the x -axis. This streak strongly indicates existence of empty voids on the interface of PP and PE. The shape of the void is flat in the yz -plane with size of ~ 10 nm.

New reflections appear on the meridian of the SAXS “edge” pattern [bars in Fig.8.5(e)]. The new PE lamellae are developed 30 nm, whose lamellar normal parallel to the z -axis. The corresponding reflection also appears on the SAXS “through” pattern [Fig.8.5(d)]. The four-point pattern, appeared during *in situ* measurements [Figs.8.4(e) and (f)], becomes diffuse in Fig.8.5(d) by the cooling to room temperature.

8.4 Mechanism of epitaxial crystallization in the bulk sample

On the interfacial plane, $(hk0)$ planes of PP crystal are facing to PE. After melting the PE molecules, possible epitaxy starts on the PP $(hk0)$ planes. Considering the crystalline

packing of the α -PP, (100) plane has mixed right- and left-turn helices, while (010), (110) planes have molecules with the same turn. The surface of the PP crystal has regular rows of methyl groups in the (010) and (110) planes [5, 7]. These rows will cause molecule-row matching at the PP-PE interface as shown in Fig.8.2.

Angles of possible rows with the z-axis and the pitch width are determined by the crystalline structure of α -PP. The results are summarized in Table 8.1. Considering the PE crystalline planes, epitaxy on α -PP (010) plane (angle 50° , width 0.505 nm: Ep1) is the best fitting with a PE(010) plane (width 0.496 nm). The additional PE epitaxy on the PP (110) plane (angle 57° , width 0.54 nm: Ep2) is also possible.

Our experimental result indicates that PE molecules are inclined by 54° from the z-axis. It is possible to explain that the PE will be grown by mixture of the above two epitaxies (Ep1+Ep2) with the c-axis oriented PP rows. In the case of PE epitaxy with the a^* -oriented PP, the inclination angle of PE will change by 90° , resulting 40° (Ep1) and 33° (Ep2) with the z-axis. Then the averaged angle must approach to 45° . The experimental result confirms that PE molecules are mainly grown by the epitaxy with the c-axis oriented PP.

Table 8.1 Possible epitaxial rows on the α -PP planes

PP crystal plane	Angle of rows ($^\circ$)	Width of rows (nm)
010	40	0.42
010	50	0.50
110	57	0.54
110	62	0.57

When the PE epitaxy develops along the interfacial plane, the bc -plane becomes parallel to the yz -plane. Then, the a -axis is oriented along the x -axis, as revealed in Figs.8.5(b) and (c). The result shows the same phenomenon observed by TEM.

However, in the multilayered film, the PE (020) reflection in Figs.8.4(b), (c) and Fig.8.5(a) indicates a broad arc showing random orientation of the b -axis. This mechanism seems to occur by an additional process due to the bulk effect. Starting from the epitaxial nucleation, the PE crystal develops not only along the yz plane but also parallel to the x -axis. This phenomenon is called transcrystallization. The broad arc in the WAXS through pattern suggests that the direction of the crystalline axes is disturbed by the transcrystallization.

Considering the transcrystallization of PE, the most probable case is parallel arrangement of PE and PP, which is consistent to the results in Figs.8.5 (d) and (e) (bars and arrows). In the bulk sample, the new lamellae are developed perpendicular to the interfacial plane by the transcrystallization. The present results are summarized as follows:

- 1) *In the multi-layered PP-PE sample, the epitaxial growth of PE appears on the 010 and 110 planes of α -PP crystal. The average PE molecule are inclined by 54° from the z-axis.*
- 2) *The epitaxial PE develops along the interfacial plane in the same way observed by TEM.*
- 3) *Additional transcrystallization, perpendicular to the interface, will occur in the bulk sample.*
- 4) *PE molecules are mainly developed by the row structure of the c-axis oriented PP.*

References

1. G. Broza, U. Rieck, A. Kawaguchi and J. Petermann, *J. Polym. Sci. Polym. Phys.* **23**, 2623 (1985)
2. B. Lotz, J. C. Wittmann, *Makromol. Chem.* **185**, 2043 (1985)
3. S. Yan, J. Petermann and D. Yang, *J. Polym. Sci. Polym. Phys.* **35**, 1415 (1997).
4. S. Yan, D. Yang and J. Petermann, *Polymer*, **39**, 4569 (1998).
5. S. Yan, F. Katzenberg and J. Petermann, *J. Polym. Sci. Polym. Phys.* **37**, 1893 (1999).
6. S. Yan, F. Katzenberg, J. Petermann, D. Yang, Y. Shen, C. Straupe and J. C. Wittmann, *Polymer*, **41**, 2613 (2000).
7. S. Yan, T. Späth and J. Petermann, *Polymer*, **41**, 4863 (2000)
8. S. Yan and J. Petermann, *Polym. Bull.* **43**, 75 (1999).
9. Y. Fujiwara, *Kolloid-Zeit, Zeit. für Polym.* **226**, 135 (1968).
10. Y. Xu, T. Asano, A. Kawaguchi, U. Rieck, and J. Petermann, *J. Mater. Sci. Lett.* **8**, 675 (1989)
11. Y. Xu, T. Asano and J. Petermann, *J. Mater. Sci.*, **25** 983 (1990)
12. T. Asano, S. Yan, J. Petermann, S. Yoshida, N. Tohyama, K. Imaizumi and T. Sugiyama, *J. Macromol. Sci., B-Physics*, **B42**, 489 (2003)
13. J. Petermann and R. M. Gohil, *J. Mater. Sci.*, **14**, 2260 (1979)